Application of a simple model using UAV imagery to determine the evapotranspiration of *Cannabis sativa* L., KwaZulu-Natal Midlands, South Africa

G.M. Denton[1], S. Gokool[2], A. Clulow[1] & T.R. Hill[3*]
[1] Discipline of Agrometeorology, School of Agriculture and Science, University of KwaZulu-Natal, South Africa
[2] Centre for Water Resources Research, School of Agriculture and Science, University of KwaZulu-Natal, Pietermaritzburg 3209, South Africa

[3] Discipline of Geography, School of Agriculture and Science, University of KwaZulu-Natal, South Africa

[*]Corresponding author hillt@ukzn.ac.za
https://dx.doi.org/10.4314/sajg.v14i2.11

Abstract

The recognition of Cannabis sativa L., as a high-value crop, combined with anecdotal evidence of its successful cultivation, has led to suggestions of its significant potential for small-scale emerging farmers in rural areas of KwaZulu-Natal, South Africa. However, to ensure the feasibility and sustainability of this activity, it is necessary to investigate its impact on water resources in areas that are already water-scarce. The South African National Water Act (No. 36 of 1998) mandates the regulation of land-based activities that reduce streamflow by declaring the crop as a streamflow reduction activity (SFRA). Although hemp is recognised as a water-intensive crop, there are few field-based measurements of its evapotranspiration (ET) in South Africa. A remote sensing modelling approach was employed to evaluate the topographic effect of hemp on water usage in KwaZulu-Natal by extrapolating data from measuring points. This method used multispectral (including thermal) drone imagery to estimate ET. The QWaterModel analysed thermal images of hemp acquired from an Unmanned Aerial Vehicle (UAV) over a single growing period of the crop. QWaterModel estimates of ET (ET_{QW}) were compared to ET estimates obtained through eddy covariance −the ET_{EC} method. A total ET_{QW} of 24.2 mm was modelled, while the measured 16.9 mm for the same five days over the growing season. The variation was found to correspond well with the Normalized Difference Vegetation Index (NDVI), which was derived from the multispectral imagery. However, the ET_{QW} estimates at the beginning of the season and after harvest were more representative of the surrounding soil surfaces and grass cover than of the hemp plants. A strong correlation was observed between the ET_{QW} and the ground-based measurements. The lack of canopy closure affected the ET estimates as the single-source QWaterModel is unable to differentiate between heterogeneous canopies.

1. Introduction

Cannabis sativa L. is used in a diverse array of industries, including, as a medicine, fibre, food, or fuel (Adesina *et al*., 2020). It has been applied in fields of study as diverse as phytoremediation and carbon sequestration, and is considered to have scope for its environmental benefits. *C. sativa* L. can be subdivided into two subspecies depending on their chemical composition. This ultimately affects the use of the plant. If the delta-9-tetrahydrocannabinol (THC) content of the plant is less than 0.3%, the plant is classified as 'hemp'; if the THC content exceeds 0.3%, the plant is classified as 'marijuana' (Wimalasiri *et al*., 2021). Despite its potential benefits, it has been referred to as a water-thirsty crop (Ashworth & Vizuete, 2017), however, the evapotranspiration (ET) of *C. sativa L* remains largely unknown (Ashworth and Vizuete, 2017), with few water-use estimates available in international literature. Bauer *et al*. (2015) stated that a single *C. sativa* L. plant uses approximately 22.7 litres of water a day over a growing season in California, USA.

Evapotranspiration is described as the loss of water from the earth's atmosphere through the combined processes of evaporation from bare soil, open water bodies, and plant surfaces, and transpiration from any organic material containing moisture (Li *et al*., 2009). It is the most important flux component of the water cycle in arid and semi-arid regions (Oki & Kanae, 2006). However, the direct measurement of ET at a high temporal resolution using Eddy Covariance (ET_{EC}) methods can be time-consuming and expensive (Brenner *et al*., 2017); furthermore, it involves a single-point measurement constrained to a limited flux footprint (Burba, 2021). Since the process of ET estimation depends on site-specific soil, hydrological, plant-physiological, and meteorological variables, field equipment to estimate ET is expensive and allows for point measurements only. Internationally recognised ET measurement systems such as eddy covariance are complex to run, and there are several uncertainties in the measured results (Blatchford *et al*., 2019). As a result, the use of unmanned aerial vehicles (UAVs) has become the recognised cost-effective way to calculate ET (Brenner *et al*. 2018; Nisa *et al*. 2021). The process entails acquiring thermal images using a UAV, processing the collected data, and importing the resultant images into a model. This approach uses remotely sensed thermal data in conjunction with computer models to simulate ET fluxes at the Earth's surface (Nisa *et al*. 2021). The main advantage of using ET results from UAVs is that they provide spatial distribution data to represent the flux footprint and its variations, instead of relying on single-point measurements. Understanding and quantifying ET is essential for improved water management and streamflow policy in countries such as South Africa, where ET is a dominant factor in the water balance.

Various single-source models, including SEBS, METRIC, SEBAL and the QWaterModel (Ellsaßer *et al*. 2020; Nisa *et al*. 2021) use simple parameterization schemes to simulate turbulent fluxes; however, these are generally less accurate than dual-source models such as

TSEB and ALEXI for estimating thermal fluxes(Kustas & Norman, 1999; Verhoef *et al*., 1997). On the other hand, dual-source models are more complex and often require additional input parameters such as canopy cover. However, they are not easily available, , thereby preventing the application of these models (Ellsaßer *et al*., 2020). Single-source and dual-source models are differentiated by their approach to surface representation. A single-source model considers the surface as a uniform entity with a closed canopy cover, whereas a dual-source model differentiates between fluxes originating from the soil surface and vegetative cover (Hoffmann *et al*. 2016; Xia *et al*. 2016). Some of the most commonly used single-source models available have been reviewed by Thevs and Nowotny (2023). Although the applications of remote sensing activities have increased over recent years, modelling applications involving the ET of hemp are lacking. In fact, more recent studies using remote sensing techniques have focused on hemp phenology (Cosentino *et al*., 2012) and photosynthesis (Tang *et al*., 2018).

One such remote sensing model, QWaterModel − an open-sourced single-source energy model (Ellsaßer *et al.* 2020) − is a modification of the DATTUTDUT (Deriving Atmospheric Turbulent Transport useful to Dummies using Temperature) model (Timmermans *et al*. 2015). It is equipped to deal with cloudy conditions, since the DATTUTDUT model can only be used in clear weather. The QWaterModel assumes that ET is low when high leaf surface temperatures are measured (hot pixels), and ET is high when cooler leaf surface temperatures are measured (cold pixels) (Ellsaßer *et al.,* 2020). Simply put, the QWatermodel calculates ET (ET_{QW}) by using a set of parameters and sun-earth geometrics to solve the radiation budget (Timmermans *et al.* 2015) and produce an evaporative fraction (EF) that is scaled between the hottest pixels (zero ET) and the coldest pixels (maximum ET) in an image, known as the wet and dry limit, which is used in the upscaling of hourly ET to daily ET.

Owing to its operational simplicity, the QWaterModel was selected to assess the spatial variability of ET over a new crop type (*C. sativa L*). An EC system at the site supplied the inputs for the required model parameters over the same time frame. Thermal images were captured periodically throughout the growing season, and the ET for *C.s sativa L* grown in the KwaZulu-Natal Midlands was estimated and compared to the ET_{EC} values obtained from field trials conducted at the same location and over the same period.

2. Method

2.1. Study Site

The study was conducted on a commercial farm located approximately 20 km from Pietermaritzburg (29º31’37.0” S, 30º28’03.2” E) in the KwaZulu-Natal Midlands, South Africa. Approximately seven hectares (7 ha) was planted to hemp. Crop management was undertaken by the local farming business and included weeding, irrigation, and fertigation. An

electric fence surrounding the field, with an overnight guard present, ensured the security of the research site. The hort grass and weed covers established in the tramlines were regularly mown to reduce competition. The trial site was divided into three fields (North, East, and South), each approximately 2.5 ha in size, with the North and East fields planted with hemp clones, and the South field with feminized hemp seedlings. Eddy covariance instrumentation was set up in the South field.

The seedlings and clones were germinated in a greenhouse before being transplanted in late November 2022. The seedlings were transplanted in the South field, while the clones were assigned to the East and North fields. Drip irrigation was implemented along the drip lines, with individual drippers positioned 0.05 m from each plant stem to minimise the risk of stem rot. Fertigation was delivered through these drip irrigation lines. Each plant was spaced two metres apart, with an inter-row spacing of 2.5 m. Every fifth row was left fallow as a tramline to allow tractors to move across the field when spraying. The plants in the South field were 'topped' and their apices removed to slow their vertical growth and encourage branching. This management strategy encourages a higher concentration of flowers to form before being harvested.

2.2. Image acquisition and data processing

Every two weeks, at the beginning of the season (when weather and logistics allowed), a UAV (DJI Matrice 300; Plate 1), with a multispectral camera (MicaSense Altum, Seattle, USA) attached, was flown over the research site This exercise started one month after planting and was followed every four weeks during the second half of the season. In all, five flights were performed at an altitude of 100 m, which allowed the UAV to fly across the entire area on four fully charged batteries, with provision also being made for a small enough ground surface distance per pixel (0.07 m) for easy identification of individual plants and inter-row spaces. The irregularity of time between flights during the first half of the season and the irregularity of time of day in this research was due to variations in the weather conditions.

Plate 1: DJI Matrice 300 series drone with mounted MicaSense Altum camera used for imagery acquisition over the growing season

Raw images of each flight were imported into PIX4DFields to form an orthophoto of the research site with a resolution of 0.07 m/pixel. After the orthomosaic image was clipped to the boundaries of the hemp field, the thermal index and NDVI layers were obtained from the orthophoto; the thermal layer was then imported into the QWaterModel (version 1.5) − a plugin within the QGIS platform (version 3.28). Both NDVI and ET_{QW} maps had a resolution of 0.07 m/pixel. The model was run for each flight with in-field measurements for short-wave irradiance (W m^{-2}), net radiation (W m^{-2}), ground heat flux (percentage of net radiation) and ambient air temperature (Kelvin)[1]. As defined by Timmermans *et al.* (2015) and recommended by Ellsaßer *et al*., default atmospheric transmissivity, atmospheric emissivity, and surface emissivity (0.7, 0.8, and 1.0, respectively) were used (2020). The model calculated the minimum and maximum temperature parameters automatically, with the highest temperatures corresponding to the hottest pixels in the image. To avoid the effects of extreme outliers, such as open water bodies, the minimum temperature was defined as the value above the 0.5% lowest temperature in the image (Timmermans *et al.,* 2015).

Once the QWaterModel had been run, the latent heat flux and EF outputs for each flight were determined from the model printout and multiplied together to calculate the hourly ET_{QW}. Since the EF is assumed to remain constant during the day (Hoedjes *et al*., 2008), the upscaling

[1] These parameters were acquired from the eddy covariance system on the ground within the trial site over the same period.

of hourly ET_{QW} to daily ET_{QW} was performed by multiplying the hourly ET_{QW} by the number of hours of evaporation per day (twelve hours).

3. Results

The QWaterModel (Figure 1 and Table 1) overestimated the accumulated ET_{QW} from thehemp crop for the five-day period over which the images were captured. It predicted an accumulated ET_{QW} of 24.2 mm, while the EC system measured a total ET_{EC} of 16.9 mm over the same days. This overestimation was noted daily in four of the five non-consecutive measurement days. Compared to the EC system, the ET_{QW} results for the final flight of the season were the most similar, although the ET_{QW} was lower than ET_{EC} on day 124. On growth day 30 (27 December 2022), the QWaterModel estimated a daily ET of 7.7 mm *versus* the 3.9 mm from the EC system. On day 124 (31 March 2023), the QWaterModel underestimated ET at 1.1 mm, while the eddy covariance system measured 2.2 mm.

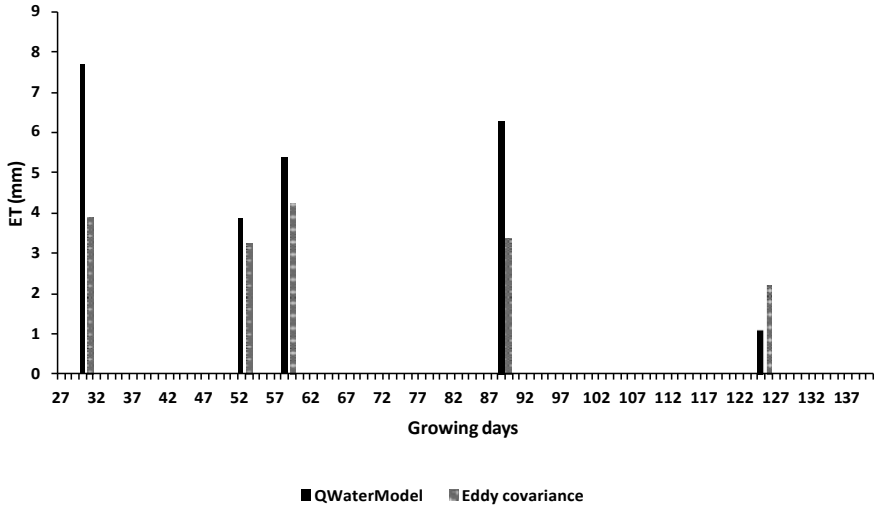

Figure 1: Modelled evapotranspiration using the QWaterModel against measured evapotranspiration using an eddy covariance system (December 2022 – April 2023)

Table 1: ET comparison between QWaterModel ET (ET_{QW}) and ground-based eddy covariance measurements

Date	ET_{QW} (mm)	EC (mm)
27 December 2022	7.7	3.9
18 January 2023	3.9	3.3
24 January 2023	5.4	4.2
23 February 2023	6.3	3.4
31 March 2023	1.1	2.2

Based on a PIX4DFields Digital Elevation Model (DEM), the average height of the study site ranged from approximately 856 m above sea level on the western side of the field to 864 m on the eastern side. As a result, ET_{QW} was higher on the western side of the field (Figure 2). Being influenced by the surrounding weeds, grasses and bare soil, ET_{QW} was clearly influenced by the topography. The Normalised Difference Vegetation Index (NDVI) was compared to ET_{QW} for each flight in December 2022 (Figure 2a), early January 2023 (Figure 2b), late January 2023 (Figure 2c), February 2023 (Figure 2d), and March 2023 (Figure 2e). Areas with high NDVIs (hemp plants and weeds in the tramlines) were observed to have a higher ET_{QW}, while those with low NDVI values (bare soil) had low ET_{QW} values. These distinctions are clearly observed between rows, where increased canopy cover from the surrounding short grass cover would likely lead to increased transpiration. This can be observed in Figure 2d, just before harvest, where the hemp plants were at their the largest, and the gaps (bare soil) between the hemp plants were more defined.

Areas of bare soil and low ET_{QW} are clearly visible in Figure 2a after planting. The soil surface in Figure 2a has a low NDVI of approximately zero (brown), whereas the weeded tramlines have an NDVI of close to one (green). The brown NDVI corresponds with the red ET_{QW} and the green NDVI with the blue ET_{QW}. The high resolution of 0.07 m/pixel made it possible to zoom in and identify the NDVI and ET_{QW} of individual plants. Figures 2b and d were both clipped as a result of a PIX4DFields processing error. The images from the flights in these two cases were reprocessed multiple times but could not be rectified. Because approximately 1.3% of Figure 2b and 0.4% of Figure 2d are missing, the influence on average ET_{QW} estimates was considered negligible.

A strong correlation between ET_{QW} and ET_{EC} was observed, with Pearson coefficient of r =

0.8 and a coefficient of determination of $R^2 = 0.67$), thereby indicating a strong linear relationship between the two variables. More validation points are recommended, however. Further correlations between NDVI and ET_{QW} were established during flights in February 2023 and March 2023, where the hemp plants could be clearly distinguished from the surrounding vegetation.

a (i)

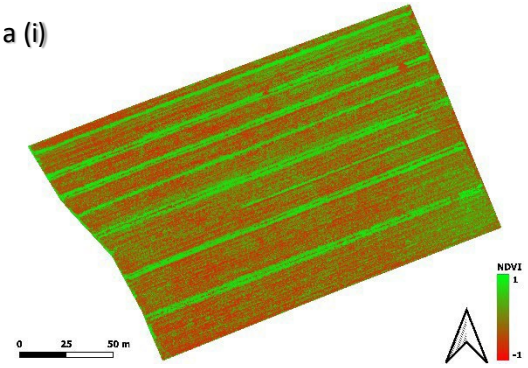

December 2022; 11:05 am

(ii)

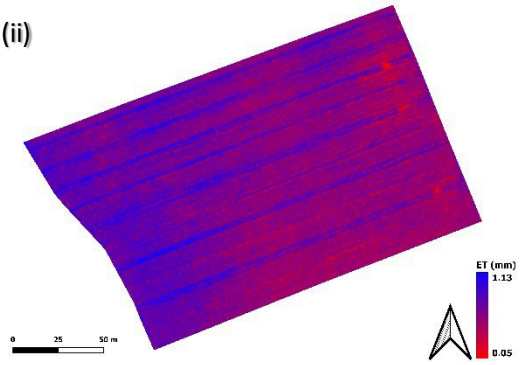

December 2022; 11:05 am

b (i)

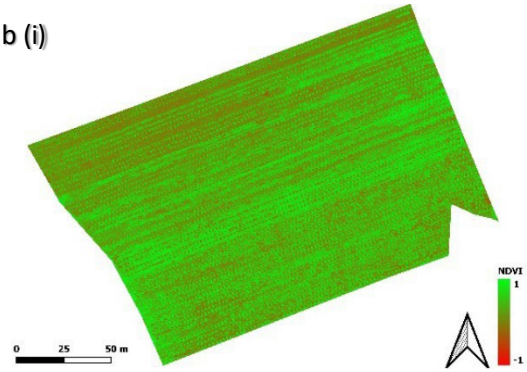

January 2023; 09:20 am

(ii)

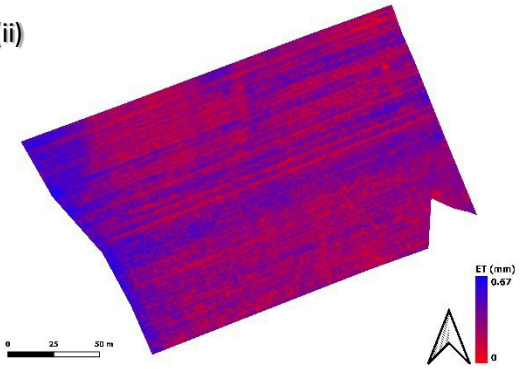

January 2023; 09:20 am

c (i)

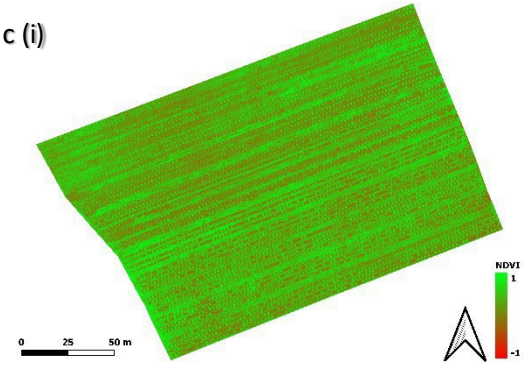

January 2023; 11:07 am

(ii)

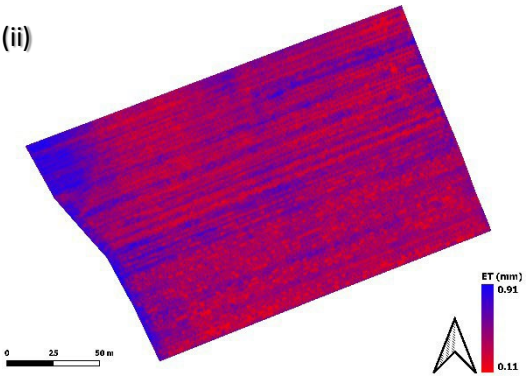

January 2023; 11:07 am

d (i)

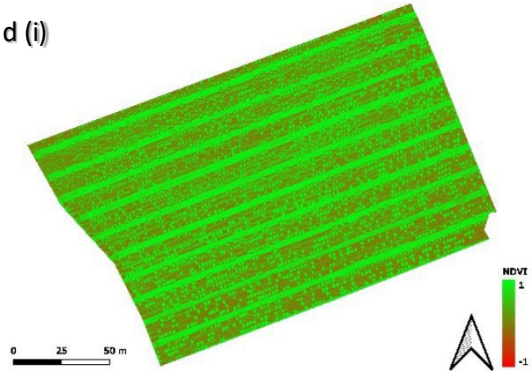

February 2023; 11:48 am

(ii)

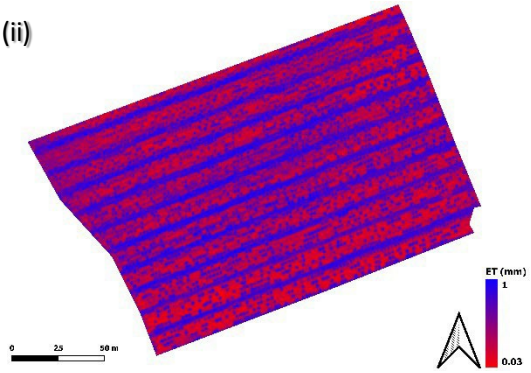

February 2023; 11:48 am

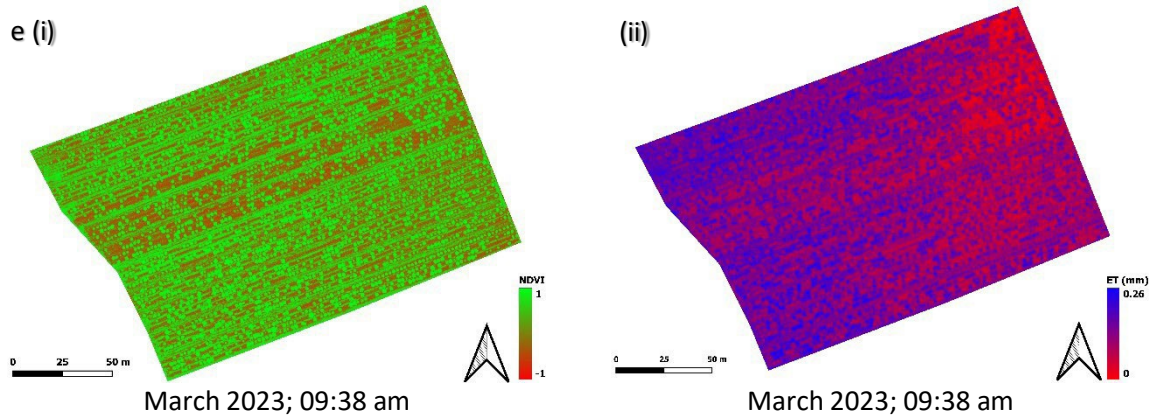

Figure 2: Comparison of (i) NDVI and (ii) QWaterModel ET throughout the growing season

4. Discussion

With the aid of drone imagery and the QWaterModel, it was possible to record variations of ET_{QW} across the field and for individual plants. These images compare water usage between the grasses and weeds in the tramlines and the hemp plants, highlighting the differences between the weeded and vegetated areas. This offers clearer insights into water consumption by hemp *versus* that for weeds and grass, an aspect that the single-point measurement of the EC system does not show. The QWaterModel overestimated ET_{QW} at the beginning of the season (growing day 30), reporting 7.7 mm/day *versus* 3.9 mm/day from the eddy covariance system. This discrepancy may be because the hemp plants were still small. As such, the ET_{QW} estimates could be influenced by the surrounding soil surface and weeds (Irmak, 2008). A lack of canopy cover, owing to the prevalence of small plants, exposes the soil surface beneath, thereby affecting the reflective spectral characteristics of the crop (Kremneva *et al*. 2023). This concurs with a statement by the QWatermodel authors, Ellsaßer *et al*. (2020), that this model performs best when ET_{QW} estimates are low, resulting in the strongest correlations between model predictions and eddy covariance measurements.

The QWaterModel lacks post-processing options, and the colour scale of the output maps could not be adjusted or standardised after the model was run. The maximum ET_{QW} for each flight is represented by the same maximum colour on the map legend, regardless of the actual ET_{QW} value. Since all the flights share the same maximum values, it is difficult to compare the maximum ET_{QW} values shown, for example, 2a (ii), c (ii), and d (ii) do not have a minimum ET_{QW} value of zero as evaporation was taking place from all areas of the field at the time of flight. The minimum value of ET_{QW} cannot, therefore, be set to zero as the lack of post-processing options prevents the colour scales of the output maps from being adjusted to accommodate these minimum values.

Although the model can be run with minimal parameters (requiring only the thermal image and the time of day), it should be noted that the model developers stated that the more input parameters used in the model, the better the performance of the model. Ellsaßer *et al*. (2020) further observed that thermal images taken around noon result in higher estimates than those issuing from the eddy covariance measurements. In the present study, flights were scheduled for 11 am on growing days 30, 58, and 88, while on days 52 and 124, flights took off at 9 am. However, on day 124, ET_{QW} was underestimated, with an estimate of 1 mm *versus* the ET estimate of 2,18 mm for the EC system.

The authors of the DATTUTDUT model, the original model on which the QWaterModel is based, stated that the DATTUTDUT model does not perform well when a partial canopy cover prevails (Timmermans *et al.* 2015). In the present study, the planting density was low, with the plants being spaced every two metres (2 m), thereby preventing full canopy closure. Furthermore, the removal of male plants from the trial site as soon as they were identified, to prevent cross-pollination, led to more gaps in the canopy and greater variability across the area. This increase in heterogeneity, resulting from the ensuing gaps in the canopy, was not intentional. It is worth noting that the time at which the ET_{QW} value is derived and upscaled to a daily value using the EF poses a potential source of error and requires further investigation.

The DATTUTDUT has been tested internationally in various parts of the world with climates similar to and dissimilar to that prevailing in this South African study. Generally, the model performed well when validated against eddy covariance measurements over grasslands in Germany (Brenner *et al.,* 2018) and vineyards in the USA (Xia *et al*., 2016). It also performed well across two studies of tropical oil palm plantations in Sumatra, Indonesia (Ellsäßer *et al*., 2020, 2021). However, these assessments conflict with the findings of Nisa *et al*. (2021), who observed that the model had a low congruency to ground-based EC measurements across a field of maize and fennel in southern Italy.

In a comparison between the DATTUTDUT model and the TSEB model, devised by Xia *et al*. (2016), the DATTUTDUT model was found to underperform since, being a single-source model, it does not consider the contributions of row and inter-row sources of temperature. The study by Xia *et al*. stated that the evaporative fraction output had a wider range than that of the TSEB model, translating to discrepancies in latent energy measurements and hence, ET_{QW} estimations. The DATTUTDUT model calculates the EF using net radiation minus soil heat flux to estimate turbulent heat fluxes. Therefore, the accuracy of net radiation and soil heat flux estimates influences the model outputs of the turbulent heat fluxes (Timmermans *et al*., 2015). However, provided that the errors of both quantities are of the same magnitude, the effect on the available energy is comparatively limited.

In the present study, net radiation and soil heat flux values for QWaterModel parameterisation were gathered during the trial from the eddy covariance system. The eddy covariance system was found to have an energy balance closure of 87%, indicating that the net radiation and soil heat flux measurements were accurate (Foken *et al*., 2010), thereby confirming the reliability of the EF. Its dependence on net radiation and soil heat flux values is a significant disadvantage of the model, as expensive equipment is required to measure these parameters, which are not commonly measured, but can be estimated.

Xia *et al*. (2016) observed that, unlike dual-source models, the DATTUTDUT model is insensitive to errors in land surface temperature. Their study found that the area and spatial resolution of Land Surface Temperature (LST) maps, which are the orthomosaic used to generate ET_{QW}, significantly influence the DATTUTDUT model results. Brenner *et al*. (2018) compared the effects of spatial resolution on the results of the DATTUTDUT and TSEB models. They observed that the latent heat flux estimates vary with changes in spatial resolution and show a tendency towards higher latent heat fluxes with higher spatial resolution. Overall, as shown by the model's sensitivity analysis, higher image resolution improves the accuracy of the EF estimates. Brenner *et al*. (2018) observed that at resolutions greater than 1 m/pixel, changes to image resolution have little to no impact on flux estimates; yet the higher the resolution, the greater the chance for the simultaneous presence of the minimum and maximum temperatures (wet and dry limits) that are essential for model calibration. In the present study, the QWaterModel's imported LST maps, output NDVIs, and ET maps were created at a resolution of 0.07 m/pixel. Therefore, as described by Brenner *et al*. (2018), flux estimates were not affected. Furthermore, this high resolution, made possible by using an UAV, allowed for the identification of individual plants, which is advantageous to farm management and allows for highly efficient control of plant growth and management.

Zipper and Loheide (2014) argued that the heterogeneity of a landscape complicates the definition of wet and dry limits. Furthermore, it hinders the applicability of these models when the surface is neither totally bare, nor fully covered by closed canopies. Generally, model flux measurements are more likely to concur with EC measurements when incorporated over a wide range of environmental conditions and over homogenous landscapes (Timmermans *et al*. 2007). However, gaps in the canopy occurred in the present study because of the removal of male plants, resulting in a heterogenous canopy structure. Since the QWaterModel defines these wet and dry limits as a percentage of the maximum and minimum temperatures derived from the LST map, rather than as physical temperature values derived from the EC system, the presence of this heterogeneous surface prevented the model from accurately determining these hydrological limits. Currently, this is no easy matter to overcome unless sterile seeds are used or seed companies can provide only female plants, for example, by initially using rearing facilities and selling only female plants.

The topographical effect on the spatial variation of ET_{QW} over the study site was observed in the QWaterModel results. According to the DEM, the western portion of the field is approximately eight metres (8 m) lower than the eastern portion, with the QWaterModel modelling higher ET_{QW} flux and NDVI values over the western portion of the field. There are various plausible reasons for this, including soil depth, water availability, and wind exposure. As the hemp crop grew, the influence of topography on ET_{QW} became more pronounced. Such changes and variations are not evident from the EC system results, which are based on point measurements and do not provide spatial information. The NDVI values for the crop helped explain the ET_{QW} results as, being among the most common indices, they reflect the volume of photosynthetically active vegetation and are often used as an indicator of the ecological state of a landscape (Phillips *et al*., 2008).

At the beginning of the season, hemp plants could not be individually identified in terms of their NDVI values, as they were too small. As such, there was no clear definition of ET_{QW} from the hemp plants themselves. Most of the ET_{QW} at this point emanated from the surrounding weeds and bare soil surface, with the soil being hotter than the canopy (Chirouze *et al*., 2014). The NDVI of every fifth row was found to be higher, as these rows were left fallow and were used as tramlines for tractors. Thus, there was a high presence of weeds and a short grass cover along these rows, thereby resulting in higher ET_{QW} values.

These rows could be removed from the calculation of NDVI; ET_{QW} would then require the QWaterModel to be run 11 times for each flight, one for every four isolated rows of plants, adding up in all to 66 model runs. This would be practical, however only if it could be automated in the future.

The effects of weeding and the mowed grass cover on ET_{QW} variability are represented in Figure 2c (i) and Plate 2. Both images were taken on the same day and show where weeding of the inter-rows and around the plants had taken place, with a short grass surface established in the tramlines. This resulted in a more uniform spatial pattern of ET_{QW} throughout the field. By the end of March, however, the NDVI for each hemp plant had become evident, with Figure 2e (i) reflecting robust plant growth. In contrast, ET_{QW} readings from the hemp plants appeared as small discrete areas (Figure 2e (ii)). The lack of canopy closure can be observed in Figures 2d (i) and e (i), where the NDVI of each plant contrasts with that of the surrounding bare soil or weed surfaces.

Plate 2: The South field (January 2023) after weeding between the plants. A grass and weed cover was established in the tramline and mown to reduce competition. (The research tower can be seen in the background.)

5. Conclusions

The QWaterModel is a modification of the DATTUTDUT model in that it uses several of the latter's coefficients and parameters, offering both effectiveness and a user-friendly interface for the implementation of the DATTUTDUT model. The QWaterModel was applied to estimate the ET of a hemp crop in the KwaZulu-Natal Midlands, South Africa, over a full growing season. These results were compared to ET measurements emanating from an EC system used at the same location and over the same period.

Compared to the role that satellites play in providing imagery, the UAV proved to be flexible in that it could be flown when needed. However, weather conditions and UAV availability were limitations that were experienced over the study period. Over the five UAV flights undertaken throughout the growing season, the QWaterModel was found to overestimate the ET_{QW} of hemp on four occasions. On the last flight, the QWaterModel underestimated ET_{QW}. Furthermore, there was a sound correlation between ET_{QW} and ET_{EC}. However, the low correlation between NDVI and ET_{QW}, means that NDVI cannot be considered the sole factor driving ET_{QW}. However, NDVI and ET_{QW} showed a similar trend over the growing season, reflecting the changes in the size of the hemp crop, weeding, and tramline grass cover. The ET maps indicate the variability of ET_{QW} across the field from west to east and capture the differences between healthy hemp plant rows and those that are weeded or unweeded. This successfully highlights the variations in water usage between the crop rows, inter-rows, and tramlines, and the fact that growers can potentially achieve significant water savings by managing the groundcover between the hemp rows, a significant

activity in water-stressed catchments. The approach offers high-resolution benefits for effective planting and crop management. However, its advanced technological requirements may restrict its use in smallholder or subsistence farming.

Since a heterogeneous landscape generates variations in its outputs when a single-source model such as the QWaterModel is applied, a low planting density and the removal of male plants tend to interrupt a full canopy closure, thereby preventing accurate estimates of ET_{QW}. This is evident from the overestimation of ET_{QW} at the beginning of the growing season. It underscores the fact that while the QWaterModel successfully demonstrated that it is useful in assessing ET in a spatial context, it is likely that a dual-source model such as the Two-Source Energy Balance (TSEB) model would perform more efficiently and generate more accurate outputs. This could be achieved by accounting for the contributions of the plant and soil surfaces individually. The occurrence of male plants in the trial was unintentional and precluded an accurate estimation of ET_{QW}. The findings of this study highlight the effectiveness of the QWaterModel in assessing the spatial variability of ET_{QW} as a user-friendly tool. However, they highlight the importance of model selection based on plant phenology.

The use of remote sensing techniques allowed for the assessment of ET variability across a field, that could not be viewed from ground level. The QWaterModel (Ellsaßer *et al.,* 2020) was used as a graphical user interface for the implementation of the DATTUTDUT (Deriving Atmosphere Turbulent Transport useful to Dummies using Temperature) model (Timmermans *et al*., 2015) and, according to international literature, has performed well. In the present study, ET_{QW} had a strong correlation with ground-based ET_{EC}, and clearly showed the spatial relationship between the Normalized Difference Vegetation Index (NDVI) and ET_{QW}. Visually, maps of ET variability would help growers to understand the hydrological dynamics of their field and aid in the management of water in water-scarce areas.

6. References

Adesina, I., Bhowmik, A., Sharma, H. and Shahbazi, A. (2020) 'A Review on the Current State of Knowledge of Growing Conditions, Agronomic Soil Health Practices and Utilities of Hemp in the United States', *Agriculture*, 10(4), p. 129. Available at: https://doi.org/10.3390/agriculture10040129.

Ashworth, K. and Vizuete, W. (2017) 'High Time to assess the Environmental Impacts of Cannabis Cultivation', *Environmental Science & Technology*, 51(5), pp. 2531–2533. Available at: https://doi.org/10.1021/acs.est.6b06343.

Bally, N., Zullino, D. and Aubry, J.M. (2014) 'Cannabis use and first manic episode', *Journal of Affective Disorders.* Elsevier B.V., pp. 103–108. Available at: https://doi.org/10.1016/j.jad.2014.04.038.

Batjes, N.H. (2004) 'SOTER-based soil parameter estimates for Southern Africa,' *ISRIC World Soil Information*, Wageningen, The Netherlands, Report. 2004/04, Oct. 2004. Available at: https://www.researchgate.net/publication/40121514.

Bauer, S., Olson, J., Cockrill, A., Van Hattem, M., Miller, L., Tauzer, M. and Leppig, G. (2015) 'Impacts of surface water diversions for marijuana cultivation on aquatic habitats in four northwestern California watersheds', *PLoS ONE*, 10(3). Available at: https://doi.org/10.1371/journal.pone.0120016.

Blatchford, M.L., Mannaerts, C.M., Zeng, Y., Nouri, H. and Karimi, P. (2019) 'Status of accuracy in remotely sensed and *in-situ* agricultural water productivity estimates: a review', *Remote Sensing of Environment*. Elsevier Inc. Available at: https://doi.org/10.1016/j.rse.2019.111413.

Brenner, C., Thiem, C.E., Wizemann, H.D., Bernhardt, M. and Schulz, K. (2017) 'Estimating spatially distributed turbulent heat fluxes from high-resolution thermal imagery acquired with a UAV system', *International Journal of Remote Sensing*, 38(8–10), pp. 3003–3026. Available at: https://doi.org/10.1080/01431161.2017.1280202.

Brenner, C., Zeeman, M., Bernhardt, M. and Schulz, K. (2018) 'Estimation of evapotranspiration of temperate grassland based on high-resolution thermal and visible range imagery from unmanned aerial systems', *International Journal of Remote Sensing*, 39(15–16), pp. 5141–5174. Available at: https://doi.org/10.1080/01431161.2018.1471550.

Burba, G. (2021) 'Eddy Covariance Method for Scientific, Regulatory, and Commercial Applications'. *LI-COR Biosciences. Lincoln, Nebraska*. Available at: www.licor.com (Accessed: 12 September 2023).

Chirouze, J., Boulet, G., Jarlan, L., Fieuzal, R., Rodriguez, J.C., Ezzahar, J., Er-Raki, S., Bigeard, G., Merlin, O., Garatuza-Payan, J., Watts, C. and Chehbouni, G. (2014) 'Intercomparison of four remote-sensing-based energy balance methods to retrieve surface evapotranspiration and water stress of irrigated fields in a semi-arid climate', *Hydrology and Earth System Sciences*, 18(3), pp. 1165–1188. Available at: https://doi.org/10.5194/hess-18-1165-2014.

Cosentino, S.L., Testa, G., Scordia, D. and Copani, V. (2012) 'Sowing time and prediction of flowering of different hemp (*Cannabis sativa* L.) genotypes in southern Europe', *Industrial Crops and Products*, 37(1), pp. 20–33. Available at: https://doi.org/10.1016/J.INDCROP.2011.11.017.

Dijkshoorn, J.A., van Engelen, V.W.P. and Huting, J.R.M. (2008). Soil and landform properties for LADA partner countries (Argentina, China, Cuba, Senegal and The Gambia, South Africa, and Tunisia). ISRIC Report 2008/06 and GLADA Report 2008/03, ISRIC – *World Soil Information and FAO*, Wageningen (23 pp with data set). Available at: http://www.isric.org/isric/Webdocs/Docs/ISRIC_Report_2008_06.pdf.

Ellsäßer, F., Röll, A., Ahongshangbam, J., Waite, P.A., Hendrayanto, Schuldt, B. and Hölscher, D. (2020) 'Predicting tree sap flux and stomatal conductance from drone-recorded surface temperatures in a mixed agroforestry system − a machine learning approach', *Remote Sensing*, 12(24), pp. 1–20. Available at: https://doi.org/10.3390/rs12244070.

Ellsäßer, F., Röll, A., Stiegler, C., Hendrayanto and Hölscher, D. (2020) 'Introducing QWaterModel, a QGIS plugin for predicting evapotranspiration from land surface temperatures', *Environmental Modelling & Software*, 130, p. 104739. Available at: https://doi.org/10.1016/j.envsoft.2020.104739. Ellsäßer, F., Stiegler, C., Röll, A., June, T., Hendrayanto, Knohl, A. and Hölscher, D. (2021) 'Predicting evapotranspiration from drone-based thermography-a method comparison in a tropical oil palm plantation', *Biogeosciences*, 18(3), pp. 861–872. Available at: https://doi.org/10.5194/bg-18-861-2021.

Foken, T., Mauder, M., Liebethal, C., Wimmer, F., Beyrich, F., Leps, J.-P., Raasch, S., De Bruin, H.A.R., Meijninger, W.M.L. and Bange, J. (2010) 'Energy balance closure for the LITFASS-2003 experiment', *Theoretical and Applied Climatology*, 101(1–2), pp. 149–160. Available at: https://doi.org/10.1007/s00704-009-0216-8.

Hoedjes, J. C. B., Chehbouni, A., Jacob, F., Ezzahar, J., & Boulet, G. (2008). Deriving daily evapotranspiration from remotely sensed instantaneous evaporative fraction over olive orchards in semi-arid Morocco. *Journal of Hydrology*, 354(1–4), 53–64. Available at: https://doi.org/10.1016/j.jhydrol.2008.02.016

Hoffmann, H., Nieto, H., Jensen, R., Guzinski, R., Zarco-Tejada, P. and Friborg, T. (2016) 'Estimating evaporation with thermal UAV data and two-source energy balance models', *Hydrology and Earth System Sciences*, 20(2), pp. 697–713. Available at: https://doi.org/10.5194/hess-20-697-2016.

Howlett, A.C., Barth, F., Bonner, T.I., Cabral, G., Casellas, P., Devane, W.A., Felder, C.C., Herkenham, M., Mackie, K., Martin, B.R., Mechoulam, R. and Pertwee, R.G. (2002) 'International Union of Pharmacology. XXVII. Classification of Cannabinoid Receptors', *Pharmacological Reviews*, 54(2),

pp. 161–202. Available at: https://doi.org/10.1124/PR.54.2.161.

Irmak, S. (2008) 'Evapotranspiration' in S.E. Jorgensen and B.D. Fath (eds), *Encyclopaedia of Ecology*. Oxford: Elsevier, pp. 1432–1438. Available at: https://doi.org/10.1016/B978-008045405-4.00270-6. Kremneva, O.Y., Danilov, R.Y., Sereda, I.I., Tutubalina, O. V., Pachkin, A.A. and Zimin, M. V. (2023) 'Spectral characteristics of winter wheat varieties depending on the development degree of *Pyrenophora tritici-repentis*', *Precision Agriculture*, 24(3), pp. 830–852. Available at:

https://doi.org/10.1007/s11119-022-09976-2.

Kustas, W.P. and Norman, J.M. (1999) 'Evaluation of soil and vegetation heat flux predictions using a simple two-source model with radiometric temperatures for partial canopy cover', *Agricultural and Forest Meteorology,* 94, pp. 13-29.

Li, Z.L., Tang, R., Wan, Z., Bi, Y., Zhou, C., Tang, B., Yan, G. and Zhang, X. (2009) 'A review of current methodologies for regional evapotranspiration estimation from remotely sensed data', *Sensors*, pp. 3801–3853. Available at: https://doi.org/10.3390/s90503801.

Nisa, Z., Khan, M.S., Govind, A., Marchetti, M., Lasserre, B., Magliulo, E. and Manco, A. (2021) 'Evaluation of SEBS, METRIC-EEFlux, and QWaterModel Actual Evapotranspiration for a Mediterranean Cropping System in Southern Italy', *Agronomy*, 11(2), p. 345. Available at: https://doi.org/10.3390/agronomy11020345.

Oki, T. and Kanae, S. (2006) 'Global Hydrological Cycles and World Water Resources', *Science*, 313(5790), pp. 1068–1072. Available at: https://doi.org/10.1126/science.1128845.

Phillips, L.B., Hansen, A.J. and Flather, C.H. (2008) 'Evaluating the species energy relationship with the newest measures of ecosystem energy: NDVI *versus* MODIS primary production', *Remote Sensing of Environment*, 112(9), pp. 3538–3549. Available at: https://doi.org/10.1016/j.rse.2008.04.012.

Ren, X., Li, G., Ding, S., Wang, J., Zhang, M., Sun, X., Zhao, Q. and Li, P. (2024) 'Applicability analysis of different evapotranspiration models for maize farmland in the lower Yellow River Plain based on eddy covariance measurements', *Ecohydrology & Hydrobiology* [Preprint]. Available at: https://doi.org/10.1016/j.ecohyd.2024.10.005.

Tang, K., Fracasso, A., Struik, P.C., Yin, X. and Amaducci, S. (2018) 'Water-and nitrogen-use efficiencies of hemp (*Cannabis sativa* L.) based on whole-canopy measurements and modelling', *Frontiers in Plant Science*, 9, p. 951. Available at: https://doi.org/10.3389/fpls.2018.00951.

Thevs, N. and Nowotny, R. (2023) 'Water consumption of industrial hemp (*Cannabis sativa* L.) during dry growing seasons (2018–2022) in NE Germany', *Journal fur Kulturpflanzen*, 75(7–8), pp. 173–
184. Available at: https://doi.org/10.5073/JfK.2023.07-08.01.

Timmermans, W.J., Kustas, W.P., Anderson, M.C. and French, A.N. (2007) 'An intercomparison of the Surface Energy Balance Algorithm for Land (SEBAL) and the Two-source Energy Balance (TSEB) modelling schemes', *Remote Sensing of Environment*, 108(4), pp. 369–384. Available at: https://doi.org/10.1016/J.RSE.2006.11.028.

Timmermans, W.J., Kustas, W.P. and Andreu, A. (2015) 'Utility of an Automated Thermal-based Approach for Monitoring Evapotranspiration', *Acta Geophysica*, 63(6), pp. 1571–1608. Available at: https://doi.org/10.1515/acgeo-2015-0016.

Verhoef, A., De Bruin, H.A.R. and Van Den Hurk, B.J.J.M. (1997) 'Some Practical Notes on the Parameter kB −1 for Sparse Vegetation', *Journal of Applied Meteorology*, 36(5), pp. 560–572. Available at: https://doi.org/10.1175/1520-0450(1997)036<0560:SPNOTP>2.0.CO;2.

Wimalasiri, E.M., Jahanshiri, E., Chimonyo, V.G.P., Kuruppuarachchi, N., Suhairi, T.A.S.T.M., Azam-Ali, S.N. and Gregory, P.J. (2021) 'A framework for the development of hemp (*Cannabis sativa* L.) as a crop for the future in tropical environments', *Industrial Crops and Products*, 172, p. 113999. Available at: https://doi.org/10.1016/J.INDCROP.2021.113999.

Xia, T., Kustas, W.P., Anderson, M.C., Alfieri, J.G., Gao, F., McKee, L., Prueger, J.H., Geli, H.M.E., Neale, C.M.U., Sanchez, L., Alsina, M.M. and Wang, Z. (2016) 'Mapping evapotranspiration with high-resolution aircraft imagery over vineyards using one-and two-source modelling schemes', *Hydrology and Earth System Sciences*, 20(4), pp. 1523–1545. Available at: https://doi.org/10.5194/hess-20-1523-2016.

Zipper, S.C. and Loheide, S.P. (2014) 'Using evapotranspiration to assess drought sensitivity on a subfield scale with HRMET, a high resolution surface energy balance model', *Agricultural and Forest Meteorology*, 197, pp. 91–102. Available at: https://doi.org/10.1016/j.agrformet.2014.06.009.